

University of Dundee

The cool and distant formation of Mars

Brasser, R.; Mojzsis, S. J. ; Matsumura, S.; Ida, S.

Published in:
Earth and Planetary Science Letters

DOI:
[10.1016/j.epsl.2017.04.005](https://doi.org/10.1016/j.epsl.2017.04.005)

Publication date:
2017

Licence:
CC BY-NC-ND

Document Version
Peer reviewed version

[Link to publication in Discovery Research Portal](#)

Citation for published version (APA):
Brasser, R., Mojzsis, S. J., Matsumura, S., & Ida, S. (2017). The cool and distant formation of Mars. *Earth and Planetary Science Letters*, 468, 85-93. <https://doi.org/10.1016/j.epsl.2017.04.005>

General rights

Copyright and moral rights for the publications made accessible in Discovery Research Portal are retained by the authors and/or other copyright owners and it is a condition of accessing publications that users recognise and abide by the legal requirements associated with these rights.

- Users may download and print one copy of any publication from Discovery Research Portal for the purpose of private study or research.
- You may not further distribute the material or use it for any profit-making activity or commercial gain.
- You may freely distribute the URL identifying the publication in the public portal.

Take down policy

If you believe that this document breaches copyright please contact us providing details, and we will remove access to the work immediately and investigate your claim.

The cool and distant formation of Mars

R. Brasser^{a,1,*}, S. J. Mojzsis^{b,c,1,*}, S. Matsumura^{d,2}, S. Ida^a

^aEarth Life Science Institute, Tokyo Institute of Technology, Meguro-ku, Tokyo 152-8550, Japan

^bDepartment of Geological Sciences, University of Colorado, UCB 399, 2200 Colorado Avenue, Boulder, Colorado 80309-0399, USA

^cInstitute for Geological and Geochemical Research, Research Center for Astronomy and Earth Sciences, Hungarian Academy of Sciences, 45 Budaörsi Street, H-1112 Budapest, Hungary

^dSchool of Science and Engineering, Division of Physics, Fulton Building, University of Dundee, Dundee DD1 4HN, UK

Abstract

With approximately one ninth of Earth's mass, Mars is widely considered to be a stranded planetary embryo that never became a fully-grown planet. A currently popular planet formation theory predicts that Mars formed near Earth and Venus and was subsequently scattered outwards to its present location. In such a scenario, the compositions of the three planets are expected to be similar to each other. However, bulk elemental and isotopic data for martian meteorites demonstrate that key aspects of Mars' composition are markedly different from that of Earth. This suggests that Mars formed outside of the terrestrial feeding zone during primary accretion. It is therefore probable that Mars always remained significantly farther from the Sun than Earth; its growth was stunted early and its mass remained relatively low. Here we identify a potential dynamical pathway that forms Mars in the asteroid belt and keeps it outside of Earth's accretion zone while at the same time accounting for strict age and compositional constraints, as well as mass differences. Our uncommon pathway (approximately 2% probability) is based on the Grand Tack scenario of terrestrial planet formation, in which the radial migration by Jupiter gravitationally sculpts the planetesimal disc at Mars' current location. We conclude that Mars' formation requires a specific dynamical pathway, while this is less valid for Earth and Venus. We further predict that Mars' volatile budget is most likely different from Earth's and that Venus formed close enough to our planet that it is expected to have a nearly identical composition from common building blocks.

Keywords: Mars, formation, Grand Tack, composition, isotopes

1. Introduction

The formation of the terrestrial planets is a long-standing problem that is gradually being resolved. The past decade has witnessed important progress towards a unified model of terrestrial planet formation. From analysis of samples of the oldest-known rocks collected on Earth and the Moon, from lunar, martian and asteroidal meteorites, as well as remote sensing studies, we now have information on the nature and timing of formation of several worlds in our solar system through combined geochemical models, elemental and isotopic abundances, and geochronology. Analysis of martian meteorites show that it formed within ~10 Myr of the start of the solar system (Dauphas and Pourmand, 2011). The chemical and mechanical closure of Earth's metallic core, as derived from the Hf-W chronometer, took place at least 20 Myr later than this (e.g. Kleine et al. (2009) and references therein). Adding these observations together leaves us with a general timeline for the formation of the terrestrial planets, and thus a foundation for computational models to explain their history.

In traditional dynamical models the terrestrial planets grow from a coagulation of planetesimals into protoplanets and subsequently evolve into a giant impact phase, during which the protoplanets collide with one other to give rise to the terrestrial worlds. Several variations of this scenario exist. The most recent of these, dubbed 'pebble accretion' (e.g. Levison et al. (2015) and references therein), postulates that the terrestrial planets grow directly from the accretion of a swarm of centimetre-sized planetesimals termed pebbles; the outcomes of the pebble accretion model are presently an area of much active research. For this work, however, we shall make use of the popular and more established *Grand Tack* model (Walsh et al., 2011).

Grand Tack relies on early gas-driven migration of Jupiter and Saturn to gravitationally sculpt the inner solid circum-solar disc down to ~1 AU after which terrestrial planet formation proceeds from solids in an annulus ranging from roughly 0.7 AU to 1 AU. Grand Tack has booked some successes, such as its ability to reproduce the mass-orbit distribution of the terrestrial planets, the compositional gradient, and total mass of the asteroid belt (Walsh et al., 2011). Its predictions for the composition of the terrestrial planets, however, have not been widely explored. Through a combination of geochemical and N-body simulations we here report what the Grand Tack models predicts for the variation in the bulk compositions of the terrestrial

*Corresponding author

Email addresses: brasser_astro@yahoo.com (R. Brasser), mojzsis@colorado.edu (S. J. Mojzsis)

¹Collaborative for Research in Origins (CRiO)

²Dundee Fellow

planets, with particular focus on Mars. The aim of this study is to constrain Mars' building blocks and whether these are identical to those of Earth's.

2. Isotopic heterogeneities

Geochemical data from martian meteorites suggests that the overall composition of Mars is unlike that of the Earth (and Moon). Early investigations into Mars' bulk composition concluded that its primary constituents are a highly reduced component devoid of most volatiles, and more oxidised material that follows CI abundances (Wänke and Dreibus, 1988); these are present in an approximately 2:1 ratio (Wänke and Dreibus, 1994). These same studies concluded that Mars accreted homogeneously, while Earth did not – cf. Dauphas et al. (2004). Based on the analysis of the isotopic variations in O, Cr, Ti and Ni in various meteorites, terrestrial and martian rocks, this composition ratio was recently revised: Mars is a mixture of carbonaceous and non-carbonaceous material, with the former contributing only 9%; for Earth the fraction is 24% (Warren, 2011). The link between isotopic anomalies and bulk composition is debated, but good cases for such a link have been made in the past (Warren, 2011; Dauphas et al., 2014, 2015). Therefore, in this study, we will follow these works and assume that isotopic anomalies are correlated to differences in bulk compositions.

The three oxygen isotope system (expressed in the conventional $\Delta^{17}\text{O} = \delta^{17}\text{O}_{\text{VSMOW}} - 0.52\delta^{18}\text{O}_{\text{VSMOW}}$ notation; the δ -notation denotes deviations in parts-per-thousand where isotopic ratios of the same element are normalised to a standard) permits discrimination between primordial nebular heterogeneities inherited during planet formation and mass-dependent planetary processes (Clayton and Mayeda, 1983). Mars is defined by oxygen that is significantly enhanced in the minor isotope (^{17}O) with respect to terrestrial and lunar values (Franchi et al., 1999; Rubin et al., 2000; Mittlefehldt et al., 2008; Agee et al., 2013; Wittmann et al., 2015), suggesting that the mixture of source components was different for Earth and Mars (Wänke and Dreibus, 1988, 1994; Lodders, 2000; Warren, 2011), which implies different source locations from within different compositional reservoirs of the solar nebula – cf. Fitoussi et al. (2016).

This conclusion is lent weight by several recent isotope studies in meteorites and in terrestrial and martian samples. The terrestrial isotopic composition of ^{17}O , ^{48}Ca , ^{50}Ti , ^{62}Ni and ^{92}Mo is best reproduced by a mixture of 90% enstatite chondrite, 7% ordinary chondrite and 2% carbonaceous chondrites (Dauphas et al., 2014). In contrast, for Mars a mixture of 45% enstatite chondrite and 55% ordinary chondrite can match its ^{17}O , ^{50}Ti , ^{54}Cr , ^{62}Ni and ^{92}Mo values (Sanloup et al., 1999; Tang and Dauphas, 2014), which is different from Earth's and thus hints at a formation region well away from that of Earth.

Here we build upon these previous studies and highlight isotopic differences between Earth (cf. Javoy et al. (2010)) and

Mars and major meteorite groups. In Fig.1 we present comparative Si vs. $\Delta^{17}\text{O}$ (top-left panel), V vs. $\Delta^{17}\text{O}$ (top-right panel), multiple-Cr (bottom-left panel), and Ti vs. Cr (bottom-right panel) isotope data for Mars vs. Earth, and when compared to various meteorite groups for which data are available and correlative to the same sample. Correlated silicon and oxygen isotopes for Mars generally match the ordinary chondrites (Georg et al., 2007; Pringle et al., 2013a), indicating there is little to no silicon in Mars' core, but Earth and Moon do not. The non-chondritic Si isotope composition of the Earth's mantle points to Si incorporation into the core (Georg et al., 2007). There is some debate in the literature regarding the source of Si fractionation. One argument revolves around nebular fractionation of SiO in fosterite at high temperature (Dauphas et al., 2015), while another suggests Si is fractionated during impact-induced evaporation rather than core formation (Pringle et al., 2014). Therefore, it is possible that the lower $\delta^{30}\text{Si}$ of Mars compared to Earth implies a more distant formation from the Sun, where temperatures were cooler. If the latter mechanism dominates then Mars' lower escape velocity compared to Earth could be the source of its lighter Si isotopic composition.

The correlated vanadium isotopic composition, expressed as $\delta^{51}\text{V}$, vs. $\Delta^{17}\text{O}$ for Mars is 5σ from terrestrial standards, which cannot be explained by metal-silicate partitioning (Nielsen et al., 2014). Both $\epsilon^{50}\text{Ti}$ and $\epsilon^{54}\text{Cr}$, as well as $\epsilon^{62}\text{Ni}$ (the ϵ -notation denotes deviations in parts-per-ten thousand normalised to another standardised isotopic ratio of the same element), reflect the presence of planetary-scale nucleosynthetic anomalies (Warren, 2011; Tang and Dauphas, 2014), while the origin of $\delta^{51}\text{V}$ variations is unknown.

The neutron-rich isotopes are suggested to have been implanted into the proto-solar disc by nearby supernovae (Qin et al., 2010), which is more effective at larger distances from the Sun, and could thus explain the $\epsilon^{54}\text{Cr}$ vs $\epsilon^{62}\text{Ni}$ trend observed across various meteorite groups (Warren, 2011). Studies have shown that, like in the O, Si and V systems cited above, major meteorite groups also possess $^{54}\text{Cr}/^{52}\text{Cr}$ vs. $^{53}\text{Cr}/^{52}\text{Cr}$ values that show clear differences from Earth (Trinquier et al., 2007, 2008; Qin et al., 2010). Of the Cr isotopes $\epsilon^{53}\text{Cr}$ is a tracer for volatility, and thus formation distance from the Sun, so that Mars' depletion in $\epsilon^{53}\text{Cr}$ relative to Earth hints at a cooler formation environment. Finally, the neutron-rich system, $^{50}\text{Ti}/^{47}\text{Ti}$ (expressed as $\epsilon^{50}\text{Ti}$ with respect to the terrestrial standard), contains anomalies comparable to the $\epsilon^{54}\text{Cr}$ values for the same meteorites and components (Trinquier et al., 2009). Hence, multiple lines of evidence show that different bulk elemental and isotopic makeups of Earth and Mars point to different accretionary histories and therefore source regions for the two planets.

In an alternative view presented by Fitoussi et al. (2016), Monte Carlo mixing models for a subset of isotopic systems can be devised that yield a singular mixture of various achondrite and chondritic components - some of which were likely comprised of compositionally-unconstrained differentiated planetes-

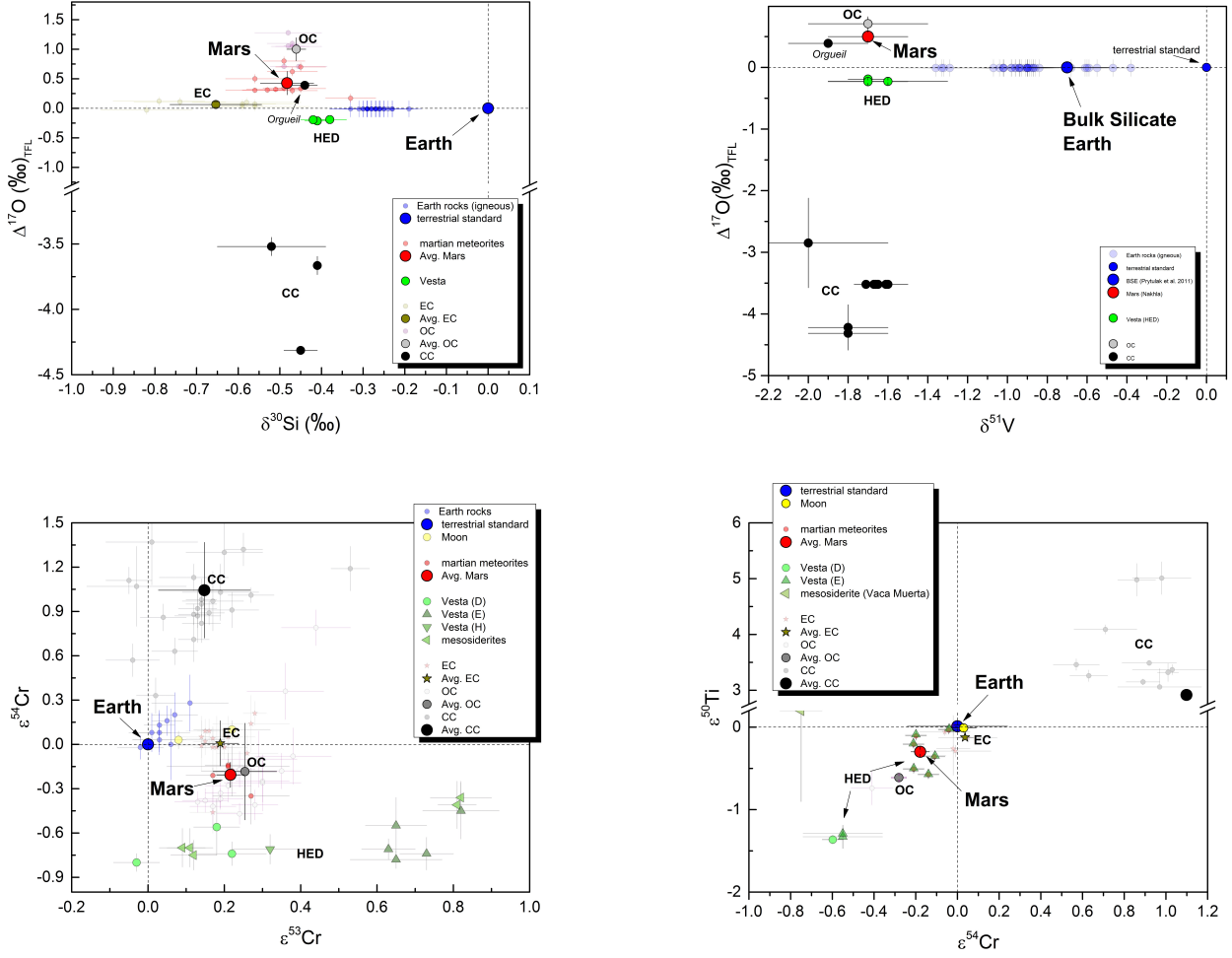


Figure 1: Four-panel plot of the correlated comparative isotopic compositions of Earth (and Moon), Mars, Vesta (howardites, eucrites, diogenites, mesosiderites), EC (enstatite chondrites), OC (ordinary chondrites), and CC (carbonaceous chondrites). All data are normalised according to the terrestrial standard values. We only plot correlated data by sample, and not just averages, for each meteorite group. As such, differences that exist between different samples in, for example oxygen isotopes in the HEDs, become highlighted. Top-left: correlated oxygen vs. silicon. Top-right: correlated oxygen vs. vanadium. Bottom-left: correlated multiple chromium isotopes (^{53}Cr and ^{54}Cr). Bottom-right: correlated titanium and chromium isotopes (^{50}Ti and ^{54}Cr).

imals - that provide an Earth and Mars bulk composition. Such Monte Carlo mixing models ultimately formulate a compositional fit for both Earth and Mars out of 10^{10} trials from 18 variables. Fitoussi et al. (2016) report that Earth and Mars are built from up to 93% of the same material. It is important to note, however, that the Monte Carlo mixing method neglects to take the dynamics of planetary formation into account. The authors state that a scenario where Mars forms beyond 2 AU is inconsistent with the outcome of their experiments and instead prefer a formation model where Mars and Earth share the same feeding zone i.e. one in which they both accrete from very similar (well-mixed) materials.

Our approach is instead to track compositions of the forming planets with dynamical simulations that yield Mars while simultaneously accounting for observational constraints. In the next section we argue for Mars' building blocks to predomi-

nantly consist of a specific mixture of meteorite parent bodies, just like most of the other terrestrial planets (Warren, 2011). We further argue from the isotope data and our dynamical simulations that bulk Mars is composed of different material than bulk Earth. Therefore Mars most likely did not form in Earth's feeding zone, and conversely grew much farther from the Sun than the Earth. This conclusion may seem obvious given the present location of Mars in the Solar System, but recent dynamical models have all but invalidated it (see Morbidelli et al. (2012) for a review). Here we show that this idea is indeed consistent with recent numerical models of terrestrial planet formation, provided that Mars followed a specific dynamical path.

3. N-body simulations and the Grand Tack

In the classical accretion model the terrestrial planets remain more or less at their current positions, with some radial

mixing caused by perturbations from the giant planets. In this model, however, the mass of Mars was always much higher than in reality (Raymond et al., 2009). A proposed solution initially confined all solid material to an annulus between the present positions of Venus and Earth at 0.7 AU and 1 AU, and with this setup the mass-distance relationship of the terrestrial planets was nicely reproduced in N-body simulations (Hansen, 2009). We refer to this model as the annulus model. A second relies on the terrestrial planets having formed from small pebbles as they spiralled towards the Sun (Levison et al., 2015), the so-called pebble accretion model. Thus, the standard model has mostly been abandoned in favour of three alternatives that confine or deliver most of the solid mass within 1 AU: the Grand Tack (Walsh et al., 2011) model, the annulus model (Hansen, 2009) and pebble accretion (Levison et al., 2015). All three can reproduce the large mass ratio between Mars and Earth. The last of these is still in its infancy, however, and the outcome of pebble accretion N-body simulations are sensitive to the underlying disc structure, leading to a great variety of outcomes (Ida et al., 2016). For this reason we make use of the Grand Tack.

Briefly, Grand Tack relies on the early, gas-driven radial migration of Jupiter. After the gas giant formed it opened an annulus in the gas disc and began migrating towards the Sun (Lin and Papaloizou, 1986) because torques acting on the planet from said disc are imbalanced. At the same time, beyond Jupiter, Saturn slowly accreted its gaseous envelope. Once Saturn reached a critical mass of about 50 Earth masses it migrated Sunward too, then rapidly caught up with Jupiter and became trapped in the 2:3 mean motion resonance (Masset and Snellgrove, 2001). This particular configuration of orbital spacing and mass ratio between the gas giants reversed the total torque on both planets, thus reversing their migration; the planets tacked. To ensure Mars did not grow beyond its current mass, the location of this tack was set at 1.5 AU (Walsh et al., 2011). The Grand Tack scenario can further account for the mass-semimajor axis distribution of the terrestrial planets and the demography of the asteroid belt (Walsh et al., 2011; DeMeo and Carry, 2014).

The dynamical consequences of the Grand Tack model on the terrestrial planet region are two-fold: First, as Jupiter migrated towards the Sun, it strongly scattered all protoplanets and planetesimals in its path. This scattering placed about half of the solid mass of the disc (equivalent to about 1.8 Earth masses) from the inner solar system to farther than 5 AU from the Sun. Second, Jupiter acted as a snowplough that pushed some protoplanets and planetesimals towards the Sun. This shepherding of material mostly occurred within the 2:1 mean motion resonance with the planet. When Jupiter reversed its migration at 1.5 AU it caused a pileup of solid material inside of 1 AU at the location of the 2:1 resonance. Thus, almost all protoplanets and planetesimals that originally formed between 1 AU and 1.5 AU were cleared by Jupiter, with a few pushed inside of 1 AU. Owing to the fact that Mars is currently at 1.5 AU from the Sun and formed farther than the Earth, it escaped Jupiters Grand Tack incursion somehow. We propose a scenario wherein proto-Mars formed in a few million years (Dauphas and Pourmand,

2011; Tang and Dauphas, 2014) farther than 1.5 AU from the Sun. The still-growing, but nearly-formed Mars subsequently migrated inwards to 1.5 AU by the dynamical interaction with Jupiter, other protoplanets and planetesimals in the disc.

To test our hypothesis we ran a high number of N-body simulations in the framework of the Grand Tack model with the tack at 1.5 AU and 2 AU. All of these simulations and the data used here are discussed in our earlier analysis of the Grand Tack model (Brasser et al., 2016). We briefly summarise our initial conditions and methods here.

The initial conditions consist of a solid disc of sub-Mars sized planetary embryos and equal-mass planetesimals, with Jupiter and Saturn situated farther out. The individual embryo masses are either 0.025, 0.05 or 0.08 M_{\oplus} . To account for the evolution of the gas in the disc during the time that the embryos form we assume a stellar age of 0.1 Myr when embryos have a mass of 0.025 M_{\oplus} , 0.5 Myr when the embryos have a mass of 0.05 M_{\oplus} and a disc age of 1 Myr when the embryos have a mass of 0.08 M_{\oplus} (Brasser et al., 2016). The ratio of the total mass in the equal-mass embryos versus planetesimals is either 1:1, 3:1 or 7:1. The planetesimals exert dynamical friction on the planets. The different total mass ratios between the embryos and the planetesimals were chosen to study how the final orbital eccentricities and inclinations of the planets depend on this initial mass ratio.

The system consisting of gas giants, planetary embryos and planetesimals is simulated with the symplectic integrator package SyMBA (Duncan et al., 1998) for 150 Myr using a time step of 7.3 days. The migration of the gas giants was mimicked through fictitious forces (Walsh et al., 2011). The gas disc model is based on that of Bitsch et al. (2014), with an initial surface density of 2272 g cm⁻². The disc's surface density at a fixed location decreases with time according to $\Sigma \propto t^{-7/5}$ (Hartmann et al., 1998). After 5 Myr, when the stellar accretion rate drops below $10^{-10} M_{\odot} \text{ yr}^{-1}$, we artificially photoevaporated the disc away exponentially with an e-folding time of 100 kyr (Bitsch et al., 2014). The planetary embryos experienced type I migration and tidal damping of their eccentricities and inclinations from the gas disc (Tanaka and Ward, 2004). The planetesimals experience gas drag, for which we assumed each planetesimal had a radius of 50 km. SyMBA treats collisions between bodies as perfect mergers, preserving their density. This works well in most circumstances, but given that all the terrestrial planets have different densities from each other and from most meteorites we modified SyMBA and implemented a mass-radius relationship that fits well through Mars, Venus and Earth (Seager et al., 2007). This relation is applied after each collision to ensure that the final planets have radii comparable to the current terrestrial planets. Initially all planetary embryos and planetesimals have a bulk density of 3 g cm⁻³.

The correlated isotope data for the various planets and meteorites, and their sources, are listed in the Supplementary Material.

The isotopic, and therefore compositional, differences between Earth and Mars can possibly be quantified by tracking the initial heliocentric distance of material that will be incorporated into the planets. Assuming that the disc follows a simple relation between isotopic ratios and distance to the Sun it is possible to crudely quantify a bulk composition for all of the planets. However there is no well-established method for doing so. For example, it has been suggested that the primordial disc was homogeneous in silicon isotopes (Pringle et al., 2013b), while there appears to be a gradient in ^{54}Cr and ^{50}Ti (Yamakawa et al., 2010), implying that several relationships ought to be used for different systems. A parsimonious approach is to assume that solar system material is increasingly oxidised with heliocentric distance, with very reduced material residing closer than 1.2 AU and more oxidised material farther out (Rubie et al., 2015). This can then be tied to the major meteorite groups. The most recent attempt, which is based on the Grand Tack model, suggested that enstatite chondrites resided between 1 AU to 2 AU, ordinary between 2 AU and 3 AU and the carbonaceous chondrites come from beyond 6 AU (Fischer-Gödde and Kleine, 2017).

Here we opt to use the composition of the asteroid belt to partition the different meteorite groups (DeMeo and Carry, 2014): enstatites originate within 1.5 AU, the ordinary chondrites resided between 1.5 AU and 3 AU and carbonaceous chondrites farther than 3 AU. In the next section we record the initial positions of embryos and planetesimals and how they assemble into the final planets. Since their initial position is a proxy for isotopic composition, we are able to characterise pathways for the Mars analogue that are consistent with its compositional affinity for ordinary chondrites, and thus quantify any compositional differences with Earth.

4. Results

We present the summary of our Grand Tack simulations with a tack at 1.5 AU in Fig. 2, which depicts the mass-weighted mean initial semi-major axis of material incorporated into the planets versus the final semi-major axis of all the resulting planets from the simulations; this encompasses the contribution from both embryos and planetesimals. The error bars are weighted standard deviations. It is clear that the majority of planets end up between 0.5 AU to 1.3 AU and they sample the region of the protoplanetary disc between 0.7 AU and 1.7 AU. This outcome is not surprising, because Jupiter’s incursion empties out the disc beyond approximately 1.2 AU while also pushing some material inwards. Planets that are situated further either escaped ejection or were tossed outward from the annulus inside of 1.2 AU. Planets situated near 1.5 AU tend to have a mass-weighted mean initial semi-major axis of 1.2 AU, but a few cases have higher values, beyond 1.5 AU. Following Brasser et al. (2016), we define a Mars analogue having a final semi-major axis between 1.3 AU and 1.7 AU. We also require that its mass $0.05M_{\oplus} < m_p < 0.15M_{\oplus}$.

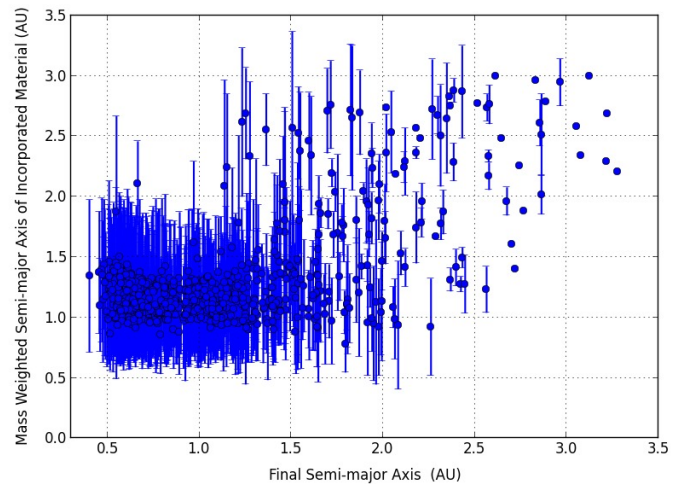


Figure 2: Mass-weighted initial semi-major axis of material incorporated into the planets as a function of their final semi-major axis. The Grand Tack clears the disc beyond 1 AU and mixes in some material from farther out, so that there are many planets that only sample the inner disc.

In Fig. 3 our extreme case yields a Mars analogue that is compositionally very different from the Earth. The final planetary system has a Mercury analogue of $0.08 M_{\oplus}$ at 0.55 AU, a Venus analogue of $0.97 M_{\oplus}$ at 0.69 AU, an Earth analogue of $0.52 M_{\oplus}$ at 1.12 AU and a Mars analogue of $0.12 M_{\oplus}$ at 1.79 AU. The left panel depicts the evolution of the semi-major axes of the terrestrial planet analogues, with the coloured dots indicating the time and initial semi-major axis of embryos and planetesimals that collided with the planets. The Mars analogue started as an embryo beyond 3 AU, and apart from a very brief excursion to the outer Solar System due to encounters with Jupiter, landed near its current location. We add that it is more typical for a distant Mars analogue to be pushed inwards through capture in the 2:1 resonance with Jupiter rather than through repeated scattering.

The right panel plots the final semi-major axis versus the mass-weighted mean initial semi-major axis of the terrestrial planet analogues. The solid error bars depict the total range of material incorporated into the final planets in the Grand Tack model while the dotted error bars are the same if we suppose the planets originated from the same narrow region between 0.7 AU and 1 AU as in the annulus model. In this simulation all material incorporated into the Mars analogue comes from beyond 2 AU in the Grand Tack case, while in the annulus model the material accreted by all planets would have originated inside of 1 AU (by definition, because initially there is no solid material beyond 1 AU). On the other hand, material accreted by the Earth and Venus analogues mostly samples the inner region of the disc for both models, suggesting a very distinct composition from the Mars analogue.

We now compare our results with those of Fitoussi et al. (2016). As mentioned above, Fitoussi et al. (2016) attempted to reproduce the composition of the terrestrial planets by sam-

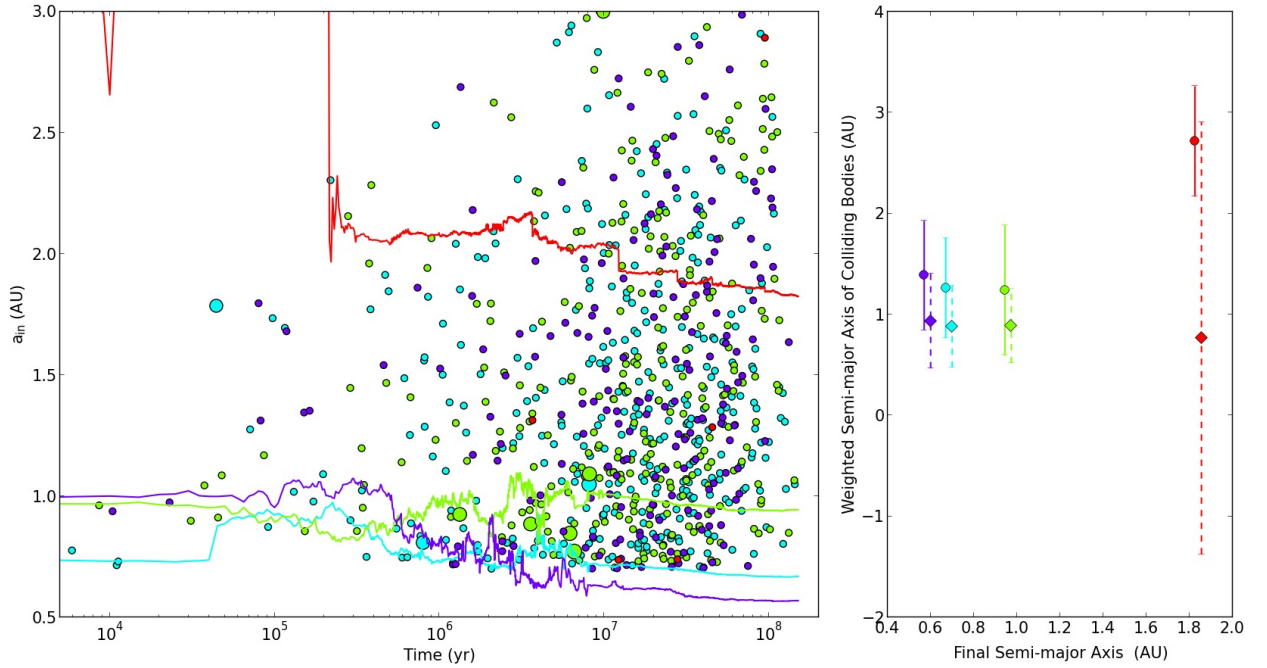


Figure 3: Dynamical evolution of an extreme case that yields a Mars analogue that is compositionally different from the Earth and Venus because it samples a distinctly different region of the protoplanetary disc. The left panel indicates the evolution of the semi-major axis of the four terrestrial planet analogues and the coloured dots indicate the initial semi-major axis and time of bodies that collide with the terrestrial planet analogues. The size of the dots is indicative of their mass. The Mars analogue gets scattered first outwards and then inwards by Jupiter and slowly migrates towards 1.8 AU through dynamical interaction with the remaining planetesimals. The right panel indicates the mass-weighted mean initial semi-major axis of material that is incorporated into the four terrestrial planet analogues. The error bars depict the total range of material incorporated into the final planets in the Grand Tack model while the dotted error bars are the same if we suppose the planets originated from the same narrow region between 0.7 AU and 1 AU as in the annulus model.

plung different source materials, reflected in different meteorite groups, from the protoplanetary nebula in a Monte Carlo approach. Fitoussi et al. (2016) conclude that Earth and Mars have a very similar bulk composition, that is both planets shared the same (mixed) source material. Such an outcome is only possible if both worlds accreted the same source material i.e. their feeding zones greatly overlapped. Dynamically the two planets can only have a nearly identical composition if they formed close to each other in a common narrow annulus of the protoplanetary disc, with Mars subsequently scattered out of the annulus to its present position, which prevented further accretion.

We present the dynamical evolution of such a case in Fig. 4, where the final planets are a Mercury analogue of $0.17 M_{\oplus}$ at 0.55 AU, a Venus analogue of $1.13 M_{\oplus}$ at 0.69 AU, an Earth analogue of $0.59 M_{\oplus}$ at 1.09 AU and a Mars analogue of $0.06 M_{\oplus}$ at 1.40 AU. Although this type of evolution where Mars originates within 1 AU and is subsequently scattered outwards is the most common, it is inconsistent with the compositional difference between Earth and Mars, not least the increased ordinary chondrite component in Mars compared with Earth. Thus, for Earth and Mars to have a very different composition we argue that Mars must have predominantly assembled from material beyond 1.5 AU, of which Earth accreted relatively little.

Under the assumption of the compositional gradient in the disc presented earlier, we find that on average the Venus, Earth and Mars analogues are composed of $82\% \pm 10\%$, $87\% \pm 8\%$ and $69\% \pm 30\%$ enstatite chondrite and $18\% \pm 10\%$, $13\% \pm 7\%$ and $31\% \pm 30\%$ ordinary chondrite. The fraction of carbonaceous chondrite is insignificant, which is most likely an artefact of our initial conditions since the solid disc only extended to 3 AU (Brasser et al., 2016). These values are in agreement within uncertainties with earlier studies (Sanloup et al., 1999; Tang and Dauphas, 2014; Dauphas et al., 2014). In Fig. 5 we show the fraction of these materials in each planet for the two simulations discussed in Fig. 3 and Fig. 4. In the top panel, corresponding to the evolution where Mars formed far, the inner three planets are dominated by enstatite chondrite material while the Mars analogue consists mostly of ordinary chondrite material (which is consistent with Fig. 1). In the bottom panel, where Mars formed closer in, all four planets have a very similar composition. This compositional homogeneity is in agreement with Fitoussi et al. (2016) but is simultaneously inconsistent with the isotopes presented in Fig. 1.

The large uncertainties in the compositional makeup of Mars imply that there is a great variety, with some cases consisting of mostly enstatite chondrite and others that are mostly ordi-

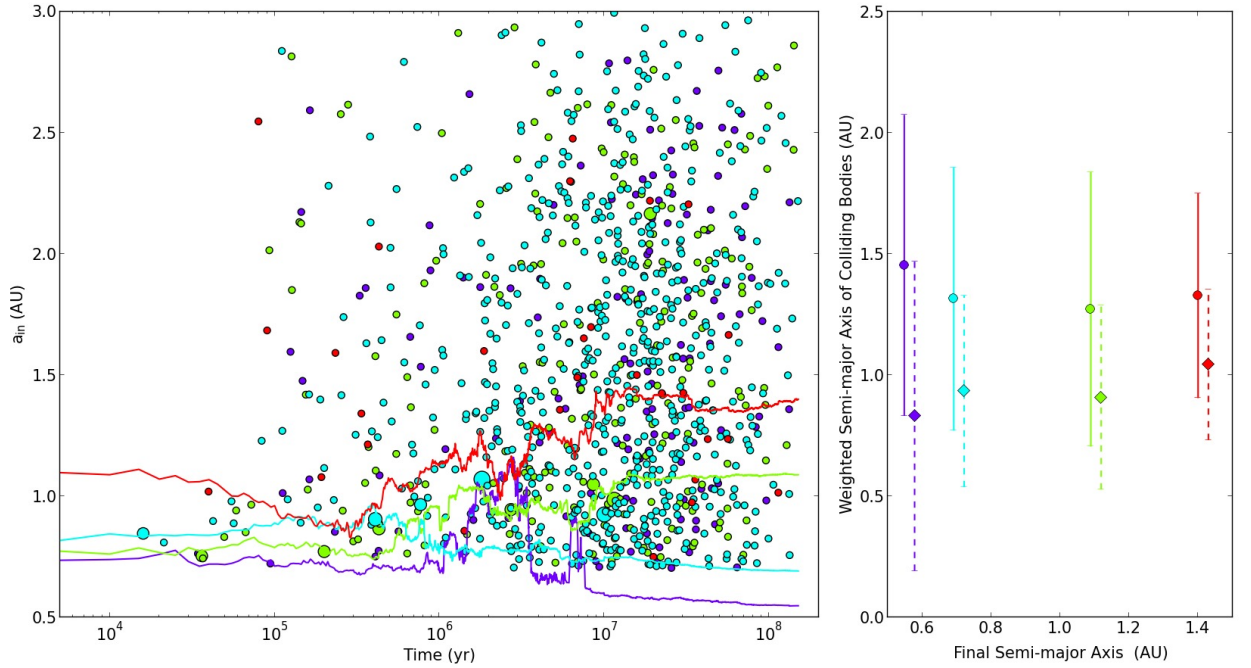


Figure 4: Same as Fig. 3 but now we show a case where the composition of the Mars analogue is nearly identical to that of the Earth analogue because they sample the same region of the protoplanetary disc.

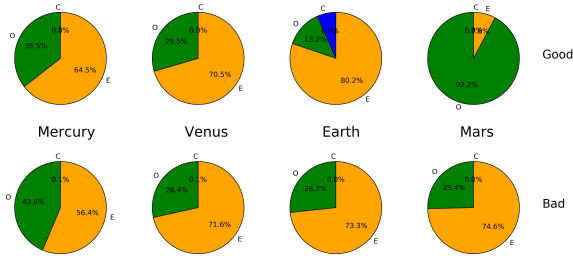


Figure 5: Pie chart of the composition of the terrestrial planets for the successful simulation, corresponding to Fig. 3 (top), and the unsuccessful simulation in Fig. 4 (bottom). Labels indicate which chart corresponds to what planet analogue. Enstatite chondrite is in orange, ordinary chondrite in green and carbonaceous in blue. In the top case the Earth analogue accreted some carbonaceous chondrite material. Note that the successful case has a composition for Mars that is strikingly different than that of the other three planets.

nary chondrite. In Fig. 6 we plot the percentage of the enstatite and ordinary chondrite components for all Mars analogues versus their initial semi-major axis. For each planet, two dots are plotted that combined add up to 100%. The transition from mostly enstatite to ordinary chondrite composition at 1.5 AU is by choice. What is important, however, is that Mars analogues that started closer than 1.2 AU have a fully mixed composition, which is expected from Fig. 2, while those that formed farther out are predominantly ordinary (beyond 1.5 AU) or enstatite (between 1.2 AU and 1.5 AU).

Fig. 7 reports our computed averages for the percentage contribution of enstatite (orange) and ordinary (green) chondrite material to the bulk chemistries of Venus, Earth and Mars. The analysis is as a function of the distance from the Sun where the dominant composition of the disc changes from one category of meteorite class to another. The error bars shown are $1\text{-}\sigma$ values. Results show that a changeover distance of 1.7 AU best matches Earth's composition of approximately 90% enstatite and 10% ordinary chondrite. This location, however, does not match Mars' 45% enstatite and 55% ordinary chondrite composition which underscores the notion that – at least for Mars – the underlying dynamics of its formation matter in its ultimate compositional make-up, as revealed in Figs. 3 and 6..

In all the various simulations performed with a tack at 1.5 AU we form a cumulative output of 635 terrestrial planets. Of these different simulations and their various outputs, a total of ten are Mars analogues with an initial semi-major axis greater than 1.5 AU. This is an effective production probability of $1.6\% \pm 0.5\%$ accounting for Poisson statistics, and as such makes this a very unlikely avenue for Mars' formation. The region of the disc beyond 1.5 AU is primarily composed of ordinary chondrite materials, which is what is likely the major constituent of Mars' bulk composition. The total fraction of Mars analogues is $8.9\% \pm 1.1\%$. Should the tack of Jupiter have occurred at 2 AU, the mass-weighted mean initial semi-major axis of planetary material versus the final semi-major axis of all the planets for the solar system would look like depicted in Fig. 8. In this

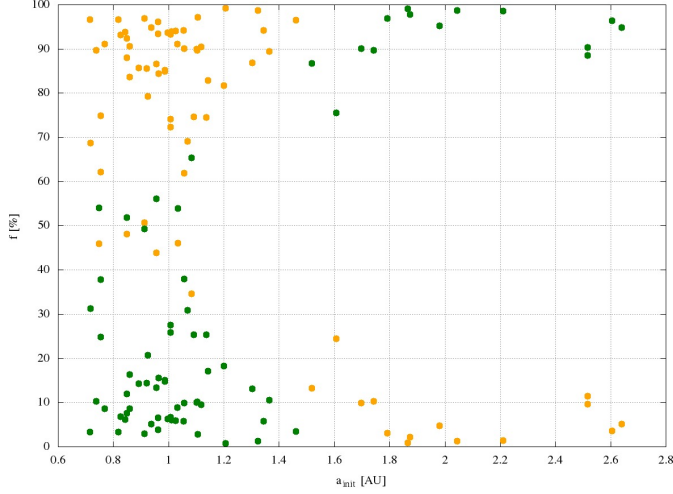


Figure 6: Scatter plot of the percentage of enstatite (orange) and ordinary chondrite (green) compositional make-up of all Mars analogues. Two dots are plotted for each planet, with the combined values adding up to 100%.

condition, there are a total of 685 planets in our cumulative output, of which just eight are Mars analogues with an initial semi-major axis greater than 1.5 AU, corresponding to a probability of $1.1\% \pm 0.4\%$. This is comparable to the case that the tack occurred at 1.5 AU. The final compositions of the planets are identical within uncertainties to the case with a tack at 1.5 AU.

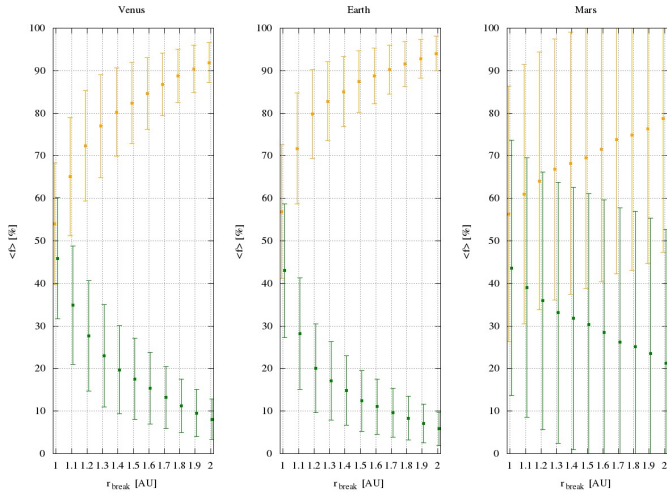


Figure 7: Scatter plot of the average percentage contribution of enstatite (orange) and ordinary chondrite (green) to the bulk compositions of Venus, Earth and Mars. Data are plotted as a function of the distance where the disc changes its composition from one meteorite class to another.

5. Discussion and Conclusions

We previously concluded that the orbital distribution of the terrestrial planets was better reproduced with a tack location of

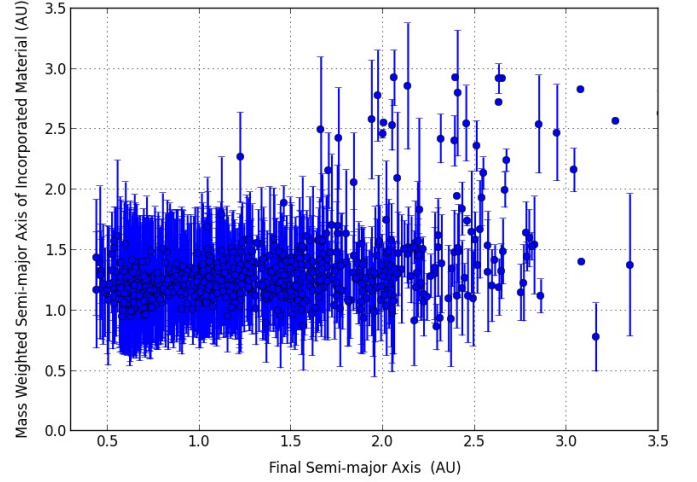


Figure 8: Mass-weighted initial semi-major axis of material incorporated into the planets as a function of their final semi-major axis for the set of Grand Tack simulations with the tack at 2 AU. Note that the majority of planets still only sample the inner part of the disc and that this region now extends to beyond 2 AU.

Jupiter at 2 AU rather than at 1.5 AU (Brasser et al., 2016). The results of the present study, on the other hand, indicate no preference. Further study on the tack location is warranted.

A more distant formation of Mars has obvious consequences beyond its bulk composition, to its proclivity to have established a biosphere. Although a topic of active debate, Mars could have retained a higher fraction of its volatile inventory than Earth (Kurokawa et al., 2014) in the absence of collisional erosion. There is no doubt that Mars was bombarded by asteroids and comets (e.g. Abramov and Mojzsis (2016)), but appears to have escaped the kind of devastating late giant impacts on the scale of which generated Earth's Moon. This separate history is consistent with analysis of martian meteorites which show relatively enhanced complements of moderately-volatile elements compared to Earth (e.g. Agee et al. (2013); Wittmann et al. (2015)), which is most probably a result of its higher fraction of ordinary chondrite material (see Supplementary materials). Delivery and retention of a hydrosphere are deemed important for a biosphere, but a consistently more distant location for Mars also calls for an historically much lower solar flux. Unless, as our model shows, an intrinsically volatile-rich Mars possessed a strong and sustainable greenhouse atmosphere, its average surface temperature was unremittingly below 0°C (Forget et al., 2013). Such a cold surface environment would have been regularly affected by early impact bombardments that both restarted a moribund hydrological cycle, and provided a haven for possible early life in the martian crust (Abramov and Mojzsis, 2016).

Our study also predicts that Venus' bulk composition, including its oxygen isotopes, should be comparable to that of the Earth-Moon system because our dynamical analyses show they share the same building blocks. Indeed, in our simulations

we find that the Venus and Earth analogues always share the same material, whereas the same cannot be said for Earth and Mars. Recent ground-based IR observations of the Venusian atmosphere yield deviations in the three-oxygen isotope system that overlap with the Earth-Moon fractionation line within errors. This is the expected result if the material that gave rise to Venus was mixed with that which built the Earth (Iwagami et al., 2015).

Given our predictions for the composition of the terrestrial planets and our simplified inverse modelling of the composition of the primordial disc, a pertinent follow-up study would consist of assuming a variety of locations of the transition from enstatite to ordinary chondrite materials and coupling this to our dynamical simulations in a Monte Carlo fashion.

6. Acknowledgements

We are grateful to A. Morbidelli, N. Dauphas and C. Burkhardt for valuable feedback during the early stages of this work. We also thank S. Charnoz and an anonymous reviewer for constructive comments that substantially improved this manuscript, and to F. Moynier for editorial assistance and for useful insights. RB is grateful for financial support from the Daiwa Anglo-Japanese Foundation and JSPS KAKENHI (16K17662). RB and SJM acknowledge The John Templeton Foundation - FfAME Origins program in the support of CRiO. SJM is grateful for support by the NASA Exobiology Program (NNH14ZDA001N-EXO).

References

- Abramov, O., Mojzsis, S. J. 2016. Thermal effects of impact bombardments on Noachian Mars. *Earth and Planetary Science Letters* 442, 108-120.
- Agee, C. B., et al. 2013. Unique Meteorite from Early Amazonian Mars: Water-Rich Basaltic Breccia Northwest Africa 7034. *Science* 339, 780-785.
- Bitsch, B., Morbidelli, A., Lega, E., Kretke, K., Crida, A. 2014. Stellar irradiated discs and implications on migration of embedded planets. III. Viscosity transitions. *Astronomy and Astrophysics* 570, A75.
- Brasser, R., Matsumura, S., Ida, S., Mojzsis, S. J., Werner, S. C. 2016. Analysis of Terrestrial Planet Formation by the Grand Tack Model: System Architecture and Tack Location. *The Astrophysical Journal* 821, 75.
- Clayton, R. N., Mayeda, T. K. 1983. Oxygen isotopes in eucrites, shergottites, nakhlites, and chassignites. *Earth and Planetary Science Letters* 62, 1-6.
- Dauphas, N., Davis, A. M., Marty, B., Reisberg, L. 2004. The cosmic molybdenum-ruthenium isotope correlation. *Earth and Planetary Science Letters* 226, 465-475.
- Dauphas, N., Pourmand, A. 2011. Hf-W-Th evidence for rapid growth of Mars and its status as a planetary embryo. *Nature* 473, 489-492.
- Dauphas, N., Chen, J. H., Zhang, J., Papanastassiou, D. A., Davis, A. M., Travaglio, C. 2014. Calcium-48 isotopic anomalies in bulk chondrites and achondrites: Evidence for a uniform isotopic reservoir in the inner protoplanetary disk. *Earth and Planetary Science Letters* 407, 96-108.
- Dauphas, N., Poitrasson, F., Burkhardt, C., Kobayashi, H., Kurosawa, K. 2015. Planetary and meteoritic Mg/Si and $\delta^{30}\text{Si}$ variations inherited from solar nebula chemistry. *Earth and Planetary Science Letters* 427, 236-248.
- DeMeo, F. E., Carry, B. 2014. Solar System evolution from compositional mapping of the asteroid belt. *Nature* 505, 629-634.
- Duncan, M. J., Levison, H. F., Lee, M. H. 1998. A Multiple Time Step Symplectic Algorithm for Integrating Close Encounters. *The Astronomical Journal* 116, 2067-2077.
- Fischer-Gödde, M., Kleine, T. 2017. Ruthenium isotopic evidence for an inner Solar System origin of the late veneer. *Nature* 541, 525-527.
- Fitoussi, C., Bourdon, B., Wang, X. 2016. The building blocks of Earth and Mars: A close genetic link. *Earth and Planetary Science Letters* 434, 151-160.
- Forget, F., Wordsworth, R., Millour, E., Madeleine, J.-B., Kerber, L., Leconte, J., Marq, E., Haberle, R. M. 2013. 3D modelling of the early martian climate under a denser CO₂ atmosphere: Temperatures and CO₂ ice clouds. *Icarus* 222, 81-99.
- Franchi, I. A., Wright, I. P., Sexton, A. S., Pillinger, C. T. 1999. The oxygen-isotopic composition of Earth and Mars. *Meteoritics and Planetary Science* 34, 657-661.
- Georg, R. B., Halliday, A. N., Schauble, E. A., Reynolds, B. C. 2007. Silicon in the Earth's core. *Nature* 447, 1102-1106.
- Hansen, B. M. S. 2009. Formation of the Terrestrial Planets from a Narrow Annulus. *The Astrophysical Journal* 703, 1131-1140.
- Hartmann, L., Calvet, N., Gullbring, E., D'Alessio, P. 1998. Accretion and the Evolution of T Tauri Disks. *The Astrophysical Journal* 495, 385-400.
- Ida, S., Guillot, T., Morbidelli, A. 2016. The radial dependence of pebble accretion rates: A source of diversity in planetary systems. I. Analytical formulation. *Astronomy and Astrophysics* 591, A72, 1-8.
- Iwagami, N., Hashimoto, G. L., Ohtsuki, S., Takagi, S., Robert, S. 2015. Ground-based IR observation of oxygen isotope ratios in Venus's atmosphere. *Planetary and Space Science* 113, 292-297.
- Javoy, M., and 10 colleagues 2010. The chemical composition of the Earth: Enstatite chondrite models. *Earth and Planetary Science Letters* 293, 259-268.
- Kleine, T., Touboul, M., Bourdon, B., Nimmo, F., Mezger, K., Palme, H., Jacobsen, S. B., Yin, Q.-Z., Halliday, A. N. 2009. Hf-W chronology of the accretion and early evolution of asteroids and terrestrial planets. *Geochimica et Cosmochimica Acta* 73, 5150-5188.
- Kurokawa, H., Sato, M., Ushioda, M., Matsuyama, T., Moriwaki, R., Dohm, J. M., Usui, T. 2014. Evolution of water reservoirs on Mars: Constraints from hydrogen isotopes in martian meteorites. *Earth and Planetary Science Letters* 394, 179-185.
- Levison, H. F., Kretke, K. A., Walsh, K. J., Bottke, W. F. 2015. Growing the terrestrial planets from the gradual accumulation of sub-meter sized objects. *Proceedings of the National Academy of Science* 112, 14180-14185.
- Lin, D. N. C., Papaloizou, J. 1986. On the tidal interaction between protoplanets and the protoplanetary disk. III - Orbital migration of protoplanets. *The Astrophysical Journal* 309, 846-857.
- Lodders, K. 2000. An Oxygen Isotope Mixing Model for the Accretion and Composition of Rocky Planets. *Space Science Reviews* 92, 341-354.
- Masset, F., Snellgrove, M. 2001. Reversing type II migration: resonance trapping of a lighter giant protoplanet. *Monthly Notices of the Royal Astronomical Society* 320, L55-L59.
- Mittlefehldt, D. W., Clayton, R. N., Drake, M. J., Righter, K. 2008. Oxygen isotopic composition and chemical correlations in meteorites and the terrestrial planets. *Reviews in Mineralogy and Geochemistry* 68, 399-428.
- Morbidelli, A., Lunine, J. I., O'Brien, D. P., Raymond, S. N., Walsh, K. J. 2012. Building Terrestrial Planets. *Annual Review of Earth and Planetary Sciences* 40, 251-275.
- Nielsen, S. G., Prytulak, J., Wood, B. J., Halliday, A. N. 2014. Vanadium isotopic difference between the silicate Earth and meteorites. *Earth and Planetary Science Letters* 389, 167-175.
- Qin, L., Alexander, C. M. O. '., Carlson, R. W., Horan, M. F., Yokoyama, T. 2010. Contributors to chromium isotope variation of meteorites. *Geochimica et Cosmochimica Acta* 74, 1122-1145.
- Pringle, E. A., Savage, P. S., Badro, J., Barrat, J.-A., Moynier, F. 2013. Redox state during core formation on asteroid 4-Vesta. *Earth and Planetary Science Letters* 373, 75-82.
- Pringle, E. A., Savage, P. S., Jackson, M. G., Barrat, J.-A., Moynier, F. 2013. Si Isotope Homogeneity of the Solar Nebula. *The Astrophysical Journal* 779, 123.
- Pringle, E. A., Moynier, F., Savage, P. S., Badro, J., Barrat, J.-A. 2014. Silicon isotopes in angrites and volatile loss in planetesimals. *Publications of the National Academy of Science* 111, 1702917032.
- Raymond, S. N., O'Brien, D. P., Morbidelli, A., Kaib, N. A. 2009. Building the terrestrial planets: Constrained accretion in the inner Solar System. *Icarus* 203, 644-662.
- Rubie, D. C., Jacobson, S. A., Morbidelli, A., O'Brien, D. P., Young, E. D., de Vries, J., Nimmo, F., Palme, H., Frost, D. J. 2015. Accretion and differentiation of the terrestrial planets with implications for the compositions of

- early-formed Solar System bodies and accretion of water. *Icarus* 248, 89-108.
- Rubin, A. E., Warren, P. H., Greenwood, J. P., Verish, R. S., Leshin, L. A., Hervig, R. L., Clayton, R. N., Mayeda, T. K. 2000. Los Angeles: The most differentiated basaltic martian meteorite. *Geology* 28, 1011.
- Sanloup, C., Jambon, A., Gillet, P. 1999. A simple chondritic model of Mars. *Physics of the Earth and Planetary Interiors* 112, 43-54.
- Seager, S., Kuchner, M., Hier-Majumder, C. A., Militzer, B. 2007. Mass-Radius Relationships for Solid Exoplanets. *The Astrophysical Journal* 669, 1279-1297.
- Tanaka, H., Ward, W. R. 2004. Three-dimensional Interaction between a Planet and an Isothermal Gaseous Disk. II. Eccentricity Waves and Bending Waves. *The Astrophysical Journal* 602, 388-395.
- Tang, H., Dauphas, N. 2014. ^{60}Fe - ^{60}Ni chronology of core formation in Mars. *Earth and Planetary Science Letters* 390, 264-274.
- Trinquier, A., Birck, J.-L., Allègre, C. J. 2007. Widespread ^{54}Cr Heterogeneity in the Inner Solar System. *The Astrophysical Journal* 655, 1179-1185.
- Trinquier, A., Birck, J.-L., Allègre, C. J., Göpel, C., Ulfbeck, D. 2008. ^{53}Mn - ^{53}Cr systematics of the early Solar System revisited. *Geochimica et Cosmochimica Acta* 72, 5146-5163.
- Trinquier, A., Elliott, T., Ulfbeck, D., Coath, C., Krot, A. N., Bizzarro, M. 2009. Origin of Nucleosynthetic Isotope Heterogeneity in the Solar Protoplanetary Disk. *Science* 324, 374.
- Walsh, K. J., Morbidelli, A., Raymond, S. N., O'Brien, D. P., Mandell, A. M. 2011. A low mass for Mars from Jupiter's early gas-driven migration. *Nature* 475, 206-209.
- Wänke, H., Dreibus, G. 1988. Chemical composition and accretion history of terrestrial planets. *Philosophical Transactions of the Royal Society of London Series A* 325, 545-557.
- Wänke, H., Dreibus, G. 1994. Chemistry and Accretion History of Mars. *Philosophical Transactions of the Royal Society of London Series A* 349, 285-293.
- Warren, P. H. 2011. Stable-isotopic anomalies and the accretionary assemblage of the Earth and Mars: A subordinate role for carbonaceous chondrites. *Earth and Planetary Science Letters* 311, 93-100.
- Wittmann, A., Korotev, R. L., Jolliff, B. L., Irving, A. J., Moser, D. E., Barker, I., Rumble, D. 2015. Petrography and composition of Martian regolith breccia meteorite Northwest Africa 7475. *Meteoritics and Planetary Science* 50, 326-352.
- Yamakawa, A., Yamashita, K., Makishima, A., Nakamura, E. 2010. Chromium Isotope Systematics of Achondrites: Chronology and Isotopic Heterogeneity of the Inner Solar System Bodies. *The Astrophysical Journal* 720, 150-154.